Characterization of the Acidic Properties of Mesoporous Aluminosilicates Synthesized from Leached Saponite with Additional Aluminum Incorporation

Thierry Linssen,*,† Filip Mees,† Kristof Cassiers,† Pegie Cool,† Andrew Whittaker,‡ and Etienne F. Vansant†

Laboratory of Adsorption and Catalysis, Department of Chemistry, University of Antwerp (UIA), Universiteitsplein1, B-2610 Wilrijk, Belgium, and Centre for High Performance Polymers, University of Queensland, QLD 4072, Australia

Received: March 12, 2003; In Final Form: June 11, 2003

The acidic properties of hexagonal mesoporous aluminosilicates synthesized via a new successful short time synthesis route using leached saponite and a low concentration of surfactant are thoroughly investigated. The resulting aluminosilicate mesoporous materials with high Si/Al ratios of around 11 have a maximal surface area of 1130 m^2/g, a pore volume of 0.92 cm^3/g, and a narrow pore size distribution at around 3 nm. The replacement of the sodium ions, present as counterions in the synthesized aluminosilicates, with protons imparts useful catalytic acidity. This acidity is extensively studied with FTIR spectroscopy after adsorption of ammonia and cyclohexylamine, while deuterated acetonitrile differentiates between Brønsted and Lewis acidity. ^{27}Al NMR spectroscopy determined the coordination of the aluminum in the FSM materials. Simultaneously the effect of an additional Al incorporation, utilizing sodium aluminate, aluminum nitrate, and aluminum isopropoxide is studied. From an acidic point of view, the incorporation with $Al(NO_3)_3$ appears to be the most optimal, as the sample has a very high amount of acid sites (1.3 mmol/g). Investigating the nature of the acid sites it is found that in all samples except the one incorporated with $Al(NO_3)_3$, more Brønsted than Lewis sites are present, both sites being quite acidic as they resist desorption temperatures up to 300 °C. Probing the coordination and location of the Al atoms, all the catalysts appeared to have mostly tetrahedral aluminum, up to 95% of the total Al amount for the proton exchanged $Al(NO_3)_3$ incorporated sample.

Introduction

The discovery of mesoporous silicates, like MCM-41 (mobil catalytic material) and FSM-16 (Folded Sheet Material), has opened the way to new zeotype molecular sieves with ordered mesoporous channel systems.[1,2] These hexagonal mesoporous materials (HMMs) have initiated a new era in the field of adsorption and catalysis, since they can be designed to have larger pore sizes than zeolites. Until the 1990s no crystalline material was synthesized possessing mesopores. FSM-16 was first synthesized by Inagaki et al. in 1993.[2] They reported the formation of a long-ranged hexagonally ordered material by an electrostatic quaternary ammonium directed rearrangement (folding) of the single-sheet silicate kanemite. However, nowadays the mechanism is thought to be different. A hexagonal structure is created by condensation of silicate, which consists of derivatives of kanemite sheets, through the formation of a mosaic of hexagonal domains.[3] Approximately at the same time researchers at Mobil reported a family of mesoporous materials (M41S) with a regular arrangement of mesopores and proposed a "liquid−crystal template" (LCT) model for the formation mechanism[1]. MCM-41, one member of this family, exhibits the same structure as FSM-16, having a hexagonal arrangement of uniform mesopores.

The purely siliceous mesoporous materials have a chemical inert silicate framework and consequently no acid sites. Since the replacement of silicon by aluminum in the framework has been reported, these materials were immediately thought to represent an extension of zeolites to carry out acid conversion of large molecules. Consequently, a large number of papers have appeared dealing with the incorporation of aluminum into the frameworks of HMMs.[4−7] Moreover, studies on the synthesis of mesoporous FSM aluminosilicates, with improved physical and chemical properties, starting from layered silicates containing aluminum are also known in the literature.[8−10] The nature of the acid sites has been extensively studied by combination of different characterization techniques such as microcalorimetry of ammonia adsorption, thermal desorption of ammonia, FT-IR spectroscopy of various probes, and ^{27}Al MAS NMR. The aluminum atoms have mainly tetrahedral configuration in the as-synthesized samples. Upon calcination, aluminum with octahedral coordination is formed, which behaves as a Lewis acid site. Brønsted acid sites are created from tetrahedrally coordinated aluminum ions by the thermal decomposition of ammonium ions generating acidic protons at the Al−O(H)−Si bridges. Brønsted acidity is an essential precondition for a variety of catalytic hydrocarbon reactions. Therefore, attempts to incorporate aluminum into tetrahedral positions of the walls of mesoprous materials have been intensified. The Si/Al bulk ratio has been varied between 100 and 10, and samples have been characterized physicochemically. Al-HMMs are catalytically active in the cracking of *n*-heptane, cumene, and vacuum gas oil.[11−13]

Very recently, for the first time, we reported on the synthesis of FSM containing framework aluminum from leached natural saponite, to obtain mesoporous materials with acidic surface

* Corresponding author. Fax: 32 3 820 2374. Tel: 32 3 8202354. E-mail: thierry.linssen@ua.ac.be.

† University of Antwerp (UIA).

‡ University of Queensland. Tel: 61 7 33654236. E-mail: andrew@cmr.uq.edu.au.

10.1021/jp034628i CCC: $25.00
Published on Web 07/19/2003

properties, in a short synthesis time (3 days instead of 15 days for the FSM synthesized from kanemite) and with a low surfactant concentration (3 wt % instead of 26 wt % for the MCM-41 synthesis).[14] These aluminosilicate mesoporous materials have a high crystallinity, pore volume, and specific surface area, creating important potential opportunities for the use as heterogeneous acid catalysts.

In current literature, there are few reports on the synthesis route starting from leached clays, although it is highly possible to obtain materials with remarkably different surface chemistry by this route. The starting clays and extent of acid leaching can affect the solid characteristics, such as the surface properties. Therefore, the physical and chemical features of these mesoporous aluminosilicates were already thoroughly investigated in a previously reported paper.[15] In this study, the influence on the acidic properties of the materials synthesized from leached clays will be investigated in detail. The acidity will be extensively studied with FTIR spectroscopy after adsorption of ammonia and cyclohexylamine, while deuterated acetonitrile will differentiate between Brønsted and Lewis acidity. ^{27}Al NMR spectroscopy will be used to determine the coordination of the aluminum in the FSM materials. Simultaneously, the effect of an additional Al incorporation, utilizing different aluminum sources, on the acidic properties of the FSM derived from saponite is studied.

Experimental Section

Materials. Saponite from near Ballarat (California, USA), supplied by the Source Clay Repository of the Clay Minerals Society is used in this work. The clay contains up to 3% diopside and tremolite, separable by wet sedimentation. Saponite, a natural trioctahedral clay with a TOT-structure, has an octahedral layer consisting of mainly $Mg(O, OH)_6$-octaheders condensed between two tetrahedral layers consisting of mainly $Si(O, OH)_4$-tetraheders. Sodium ions are located in the interlayer region to compensate for the negative charge on the sheets. The idealized chemical formula is $Na_{0.32}Ca_{0.38}(Si_{7.54}Al_{0.76})Mg_{5.22}O_{20}(OH)_4$. The exchangeable ions provide the untreated saponite a cation-exchange capacity (CEC) of 1.04 mmol/g. The size of the clay platelets used is <2 μm in diameter and 9.6 Å in height.

For the incorporation of aluminum into the structure three aluminum sources were used being, sodiumaluminate or $NaAlO_2$ (Riedel-de Haën, anhydrous, technical), aluminumnitrate or $Al(NO_3)_3$ (Fluka Chemika, 98.0%) and aluminum 2-propanol or $Al(i\text{-}C_3H_7O)_3$ (Fluka Chemika, 99%).

Quantification of the total acidity was performed via the reaction of the acid sites with ammonia or NH_3 (Praxair, anhydrous) and cyclohexylamine or CHA (Acros Organics, 99%).

Acetonitrile or CD_3CN (Acros Organics, 99 at. % D) was used to differentiate between Lewis and Brønsted acid sites.

Sample Preparation. A 2.5 g sample of the natural saponite was leached under stirring at 25 °C for 24 h by 20 mL 8 M HCl aqueous solutions to remove the magnesium containing octahedral layer. The leached silicate powders were washed and filtered several times to remove all HCl.

The aluminosilicate FSM precursors were prepared according to the method described before.[14] The leached saponite was suspended in 20 mL solution using 0.1 M cetyltrimethylammonium bromide (CTAB) as structure directing agent and 1 g of the dried leached silicate powders as silicate source, and denoted correspondingly as FSMSap. The suspension was adjusted to a pH of 12.3 with 2 M NaOH and stirred for 3 h at 70 °C. After 3 h the solid was filtered and dispersed in 20 mL distilled water, and the pH of the dispersion was adjusted to 8.5 with 2 M HCl. This suspension was stirred for a subsequent 3 h at room temperature. Additional incorporation with different aluminum sources was performed adding 0.02 g $NaAlO_2$, 0.09 g $Al(NO_3)_3 \cdot 9H_2O$, or 0.02 g $Al(i\text{-}C_3H_7O)_3$, together with the leached saponite during the first step of the synthesis, the obtained samples, respectively referred to as FSMSap $Al(NO_3)_3$, FSMSap $NaAlO_2$, and FSMSap $Al(i\text{-}C_3H_7O)_3$. All the samples were calcined at 550 °C for 6 h in air with a heating rate of 2 °C/min to obtain the mesoporous structure.

Subsequently the resulting Al-FSMSap's are converted into their acid form by extracting the Na^+ form 3 times for 2 h with a 0.5 M NH_4NO_3 solution using a liquid-to-solid ratio of 20 wt %. The NH_4^+ form was then calcined a second time at 550 °C for 6 h to obtain the acid form during the desorption of NH_3.

Characterization Methods. The chemical compositions of the samples were determined by electron probe micro analysis (EPMA) using a JEOL JCX electron microprobe analyzer. The obtained samples were stored in a nitrogen glovebox to avoid hydration until examination of their structure by X-ray powder diffraction (XRD) and N_2 adsorption. The XRD patterns were measured on a Philips PW 1840 powder diffractometer with Cu Kα radiation ($\lambda = 1.540$ Å), 45 kV, 30 mA, and a Ni filter. Nitrogen adsorption−desorption isotherms of the calcined FSM materials were recorded at 77 K on a Quantachrome Autosorb-MP automated gas adsorption system. The samples are degassed at 150 °C during 16 h in a vacuum furnace prior to analysis. Surface areas are calculated according to the BET equation, while the total pore volumes have been calculated from the adsorbed amount at a relative pressure $p/p_0 = 0.98$. Pore size distributions are obtained following the method of Barrett, Joyner and Halenda (BJH).

Quantification of the Total Acidity. To determine the total number of acid sites (mmol/g), the surface acid sites were allowed to react in a vacuum with NH_3 (1 h at 150 °C with a subsequent desorption of the physisorbed fraction via a liquid nitrogen cold trap) and CHA (1 h at ambient temperature with a subsequent heating to 150 °C at atmospheric pressure for 2 h to remove the physisorbed fraction). The amount of CHA, reacted for 1 h in a 1:1 ratio with the acid sites, was determined with thermogravimetric analysis (TGA) measuring the weight loss caused by the desorption of the CHA at 300 °C. TGA was performed on a Mettler TG 50/TA 3000 thermobalance controlled by a TC10A microprocessor. The samples were heated at a rate of 10 °C/min under an O_2 flow (150 mL/min.).

The CHA being desorbed at 300 °C was investigated with infrared measurements. The in situ DRIFT measurements were performed on a Nicolet Nexus 670 bench equipped with an in situ Spectra Tech High-Temperature Vacuum Chamber, controlled by a Spectra Tech Time Proportional Temperature Controller and a MCT detector. Samples were mixed with KBr (95% KBr, 5% sample). Spectra were collected in air at various temperatures starting from room temperature up to 500 °C. The resolution of the spectrum is 4 cm^{-1}.

Carbon microanalyses were carried out in a Perkin-Elmer CHN analyzer in order to verify the reliability of the TGA measurements toward the quantification of the number of acid sites.

The correctness of the determination of the total acidity via the desorption of CHA was checked with volumetric measurements of the amount of chemisorbed NH_3 on the acid sites.

Differentiation between Brønsted and Lewis Acidity. Transmission IR spectra were recorded on a Nicolet 20DXB FTIR spectrometer with a resolution of 4 cm^{-1}, using wafers

in the form of self-supporting pellets of the catalyst powder. The pellet was placed in a quartz IR cell equipped with KBr windows properly designed to carry out spectroscopic measurements at different temperatures. The cell was connected to a conventional vacuum line (residual pressure: 1×10^{-3} Pa) allowing all thermal treatments and adsorption−desorption experiments to be carried out in situ. The acid sites were studied after activation of the catalysts in situ at 200 °C, and evacuation under reduced pressure overnight (wafer of 10 mg/cm^2). To determine the acidity and the amount of either Brønsted or Lewis sites, the samples were allowed to react abundantly with the probe molecule, acetonitrile (CD_3CN), at room temperature for 1 h. IR spectra were recorded at different desorption temperatures varying from ambient temperature to 300 °C with steps of 50 °C.

^{27}Al MAS NMR. ^{27}Al NMR high-speed magic-angle spinning (MAS) spectra of the powdered samples were recorded applying a MAS spinning speed of ca. 7−8 kHz on a MSL300 spectrometer ($B_0 = 7$ T). The estimated values of the chemical shift for differently coordinated Al sites are derived from signal deconvolution. Data were not corrected for second-order quadrupole effects. To get the best fit of the Al NMR spectra, the Gauss-Lorentz ratios and the line widths of the individual signals were varied. Despite the known uncertainties caused by quadrupole coupling effects on signal intensities and the general problems connected to the deconvolution of strongly superimposed spectra, the relative portions of the differently coordinated Al species are reflected.

Results and Discussion

Synthesis of Acid Activated Al-FSMSap Materials. In accord with the preceding procedure,[14] we introduced saponite clays as silicate source in the synthesis of mesoporous aluminosilicate FSMSap samples (Al-FSMSap's). Although the transmission electron microscopy (TEM) and X-ray diffraction (XRD) observations of FSMSap pointed out the presence of a second phase, attributed to residual leached saponite,[15] these catalytically active Al-FSMSap's with low Si/Al ratios are physicochemically comparable to other AlSi-HMMs previously reported in the literature[4,6,16−19].

The counterion in the as-such synthesized aluminosilicate mesoporous materials after synthesis is sodium. The characterized Al-FSMSap's are converted into their acid form by exchanging the Na^+ ions with NH_4^+ ions to the acid (H^+) form after subsequent calcination. In comparison to the samples in the Na^+ form, the acidic Al-FSMSap materials (H^+ form) only have slightly higher Si/Al ratios, indicating that merely a negligible amount of aluminum is dissolved in the solution during the applied acidifying procedure. The diffraction patterns, shown in Figure 1A, still correspond to those of mesoporous materials with a hexagonal structure, but the peaks are less intense, pointing out a decrease in structure ordering due to the acid treatment on the FSMSap samples in water. As a result of silicate hydrolysis of the relative thin silica walls, the Si-HMMs are less stable in contact with water than the AlSi-HMMs. Due to this feature aluminosilicate materials with a low Si/Al have a significantly higher stability in water. This feature accounts for the higher stability toward the acidifying step of the Al-FSMSap's (Si/Al $\approx$ 11) synthesized in the presence of an additional aluminum source in comparison with the FSMSap (Si/Al $\approx$ 13). From a structural point of view, one can conclude that the Al-FSMSap samples in the H^+ form with a high aluminum content, synthesized with an additional aluminum source, all have a high unit cell parameter (±4.8 nm), surface area (±400 m/g), and pore volume (±0.3 cm^3/g) and a fairly narrow pore size distribution (±3 nm) (Figure 1B and Table 1). As also observed by Corma et al.,[5] sodium aluminate is a better aluminum source to use when HMM samples with low Si/Al are to be obtained, showing slightly better structural properties.

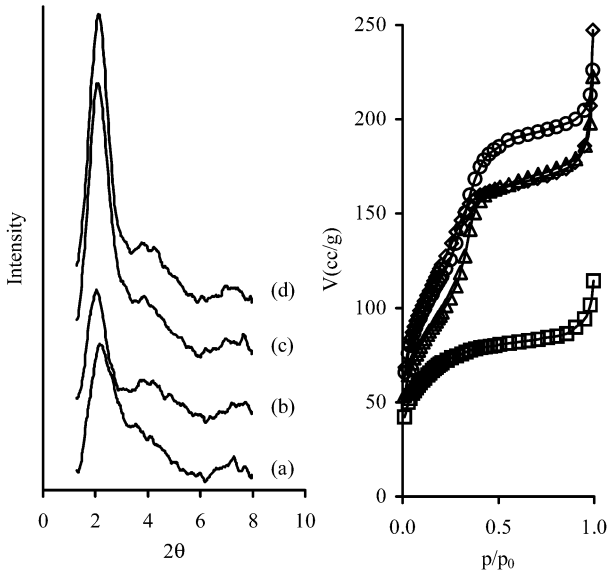

Figure 1. XRD patterns (A) and N_2 isotherms (B) of (a, □) FSMSap H^+, (b, ○) FSMSap $NaAlO_2$ H^+, (c, Δ) FSMSap $Al(NO_3)_3$ H^+, and (d, ◊) FSMSap Al(i-$C_3H_7O)_3$ H^+.

TABLE 1: Physicochemical Properties of the Al-FSMSap H^+ Samples

			N_2 adsorption data		
acidified samples (H^+)	Si/Al ratio	a[a] (nm)	S_{BET}[b] (m^2/g)	PV[c] (cc/g)	Ø[d] (nm)
FSMSap	13.2	4.5	254	0.16	2.5
FSMSap $NaAlO_2$	11.0	5.0	405	0.33	3.2
FSMSap $Al(NO_3)_3$	11.3	4.8	348	0.31	3.1
FSMSap Al(i-$C_3H_7O)_3$	11.4	4.6	441	0.32	2.9

[a] Unit cell parameter calculated from the 100 reflection of the hexagonal structure. [b] Specific surface calculated with the BET method. [c] Pore volume measured at a p/p_0 value of 0.98. [d] Mean diameter of the pore size distribution calculated with the BJH method.

Determination of the Total Acidity. The replacement of the sodium ions present as counterions in the synthesized Al-FSMSap's, first with ammonium ions and then ultimately with protons upon calcination, as was performed in the present study, imparts useful catalytic acidity. Generally the adsorption of a strong basic molecule is applied to evaluate the acidity of aluminosilicates. Strong basic molecules such as ammonia (NH_3) and cyclohexylamine (CHA) are good probes to evaluate the total acidity (Brønsted and Lewis) of AlSi-HMM materials.[20,21] The advantage of ammonia as adsorbate is the fact that NH_3 is accessible to all acid sites because of its high basicity ($pK_b = 4.75$) and little kinetic diameter ($\sigma = 2.6$ Å). CHA is an even stronger basic molecule with a pK_b of 3.34, the very weak acid sites also being titrated. The kinetic diameter of CHA is larger ($\sigma = \pm 6$ Å) compared to NH_3, resulting in the inaccessibility of the acid sites in little micropores and the lower possible loading of a surface with a large number of acid sites due to spherical constraints. As shown in the inset of Figure 2, the thermogravimetric analysis (TGA) profile for the FSMSap H^+ sample after CHA adsorption surprisingly shows only one type of acidic site in the derivative thermogravimetric analysis (DTG). The intensity of the desorption peak at 300 °C is directly

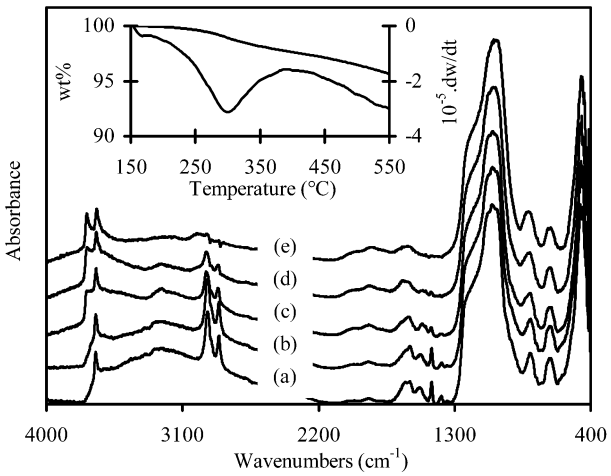

Figure 2. TGA (inset) and in situ DRIFT of FSMSap H^+ after reaction with CHA at different temperatures: (a) 25, (b) 100, (c) 200, (d) 300, and (e) 400 °C.

related to the number of aluminum centers incorporated onto the mesoporous FSMSap H^+. One could expect that the remains of the leached saponite, present beside the mesoporous material, would account for a second type of acidic site. The weight loss is induced by either the desorption or the decomposition through oxidation of the organic compounds of CHA. Therefore, with in situ Fourier transformed diffuse reflectance infrared spectrometry (DRIFT), the weight loss was identified simultaneously (Figure 2). In agreement with Lambert et al.,[22] the FSMSap H^+ sample shows two bands with different intensity ratios in the high wavenumber region. The sharp and strong band at 3734 cm^{-1} is due to isolated silanol groups (Si−OH) exposed on the external surface, while the peak at 3668 cm^{-1} is due to the octahedral Mg_3OH groups originating from the residual Saponite present after the synthesis. In spectrum a, no peak at 3734 cm^{-1} can be observed as the isolated silanols reacted with CHA. This feature already points out that this peak originates from at least weakly acidic silanol groups. Apparently the octahedral Mg_3OH groups are barely titrated by the probe molecule since almost no decrease in intensity is observed after the adsorption. This confirms that the former band is due to external OHs (silanols) available for H-bonding with CHA, while the latter is due to mostly unavailable structural "internal" OHs and a few external Mg−OHs in surface defects. The silting up of the residual clay after synthesis and the subsequent irreversible collapse of the clay after calcination could account for this feature. Around 3200 cm^{-1} a band appears that can be attributed to the bridged N−H groups. With increasing temperature this band disappears simultaneously, with the peaks corresponding to the C−H stretch vibration of the cyclohexyl group of CHA (2935 and 2858 cm^{-1}) and the symmetric and asymmetric NH_3 deformation bands of the protonated amine at respectively 1533 and 1630 cm^{-1}. The narrow band at 1452 cm^{-1} is due to the C−H bend vibration. These former bands disappear simultaneously at a temperature between 300 and 400 °C (spectrum d and e). When the decomposition of CHA would occur through oxidation of the organic compounds, the peak attributed to the vibration of the bridged N−H groups would still be visible at temperatures above 400 °C. Therefore we can conclude that the weight loss is due to the desorption of CHA and not to the oxidation of the organic components.

Taking into account the former findings, the number of acid sites for the four different Al-FSMSap H^+ samples (with and without an additional aluminum source) was calculated via the integration of the DTG curve, assuming an interaction of each basic molecule with one acid site. The acidities (mmol/g), based on the cyclohexylamine desorbed by the samples beyond 150 °C, are presented in Table 2. As a reference the quantity of chemisorbed CHA was also established via the carbon determination with a CHN analysis. The values obtained by the different methods are in good agreement for all the samples, consolidating the statement that the weight loss at 300 °C in TGA originates from the desorption of CHA. Apparently, the use of an additional aluminum source results in a significant higher number of acid sites following the order FSMSap H^+ < FSMSap $NaAlO_2$ H^+ < FSMSap Al(*i*-$C_3H_7O)_3$ H^+ < FSMSap $Al(NO_3)_3$ H^+. The incorporation with aluminum nitrate appears to be the most optimal, since the sample preserved its structure and has the lowest Si/Al ratio and the highest amount of acid sites, being 1.3 mmol/g, corresponding to approximately 3 acid sites each nm.

TABLE 2: Quantification of the Acid Sites of the Al-FSMSap H^+ Samples

acidified samples (H^+)	number of acid sites (mmol/g)		
	CHA[a]		
	TGA	CHN[b]	NH_3
FSMSap	0.25	0.27	0.29
FSMSap $NaAlO_2$	0.75	0.79	0.83
FSMSap $Al(NO_3)_3$	1.30	1.23	1.38
FSMSap Al(*i*-$C_3H_7O)_3$	0.89	0.88	0.95

[a] Determined with cyclohexylamine adsorption. [b] Carbon microanalysis.

Comparing these values with those obtained by the volumetric determination of the quantity of adsorbed ammonia on the acid sites, repeatedly a slightly higher amount of acid sites was obtained. The cause can be two-fold. First, it is possible that the acid sites in the little micropores are not accessible for the larger CHA molecule. Second, due to a heterogeneous distribution of the acid sites on the surface of the mesoporous material a part of the acid sites is not accessible because they are too close to each other resulting in the blocking of an acid site with an already adsorbed CHA molecule on a nearby acid site. Following the calculated pore size distributions, no micropores are present wherein CHA molecules with a kinetic diameter of 6 Å cannot be adsorbed. Accordingly, a little part of the acid sites is inaccessible due to mutual blocking. In Table 2 one can see that the difference in acidity obtained by adsorbing the two probes enlarge with increasing concentration of acid sites and consequently increasing chance on neighboring acid sites, consolidating the former statement.

Apparently, the quantification of the acid sites via the determination of the amount of adsorbed CHA with TGA is a reliable technique. This is certainly the case for samples with a relatively high Si/Al ratio, having only few neighboring acid sites, possibly disturbing the 1:1 ratio in the CHA adsorption. A significant advantage of this technique is the rate and the simplicity of the acidity determination.

Differentiation between Brønsted and Lewis Acidity. The nature of the acid sites on the surface of the Al-FSMSap H^+ samples was investigated by infrared spectroscopy of adsorbed deuterated acetonitrile. This probe is a weak base, and the frequency of the stretching vibration mode of the CN bond is highly sensitive to hydrogen bonding, protonation, or coordination, making it an exquisite probe for the discrimination between different acid sites.[23−25]

The regions 2200−2400 and 3000−4000 cm^{-1} of the spectra of CD_3CN adsorbed on the Al-FSMSap H^+ samples are pictured in Figure 3. Adsorption of CD_3CN on the catalysts at room-

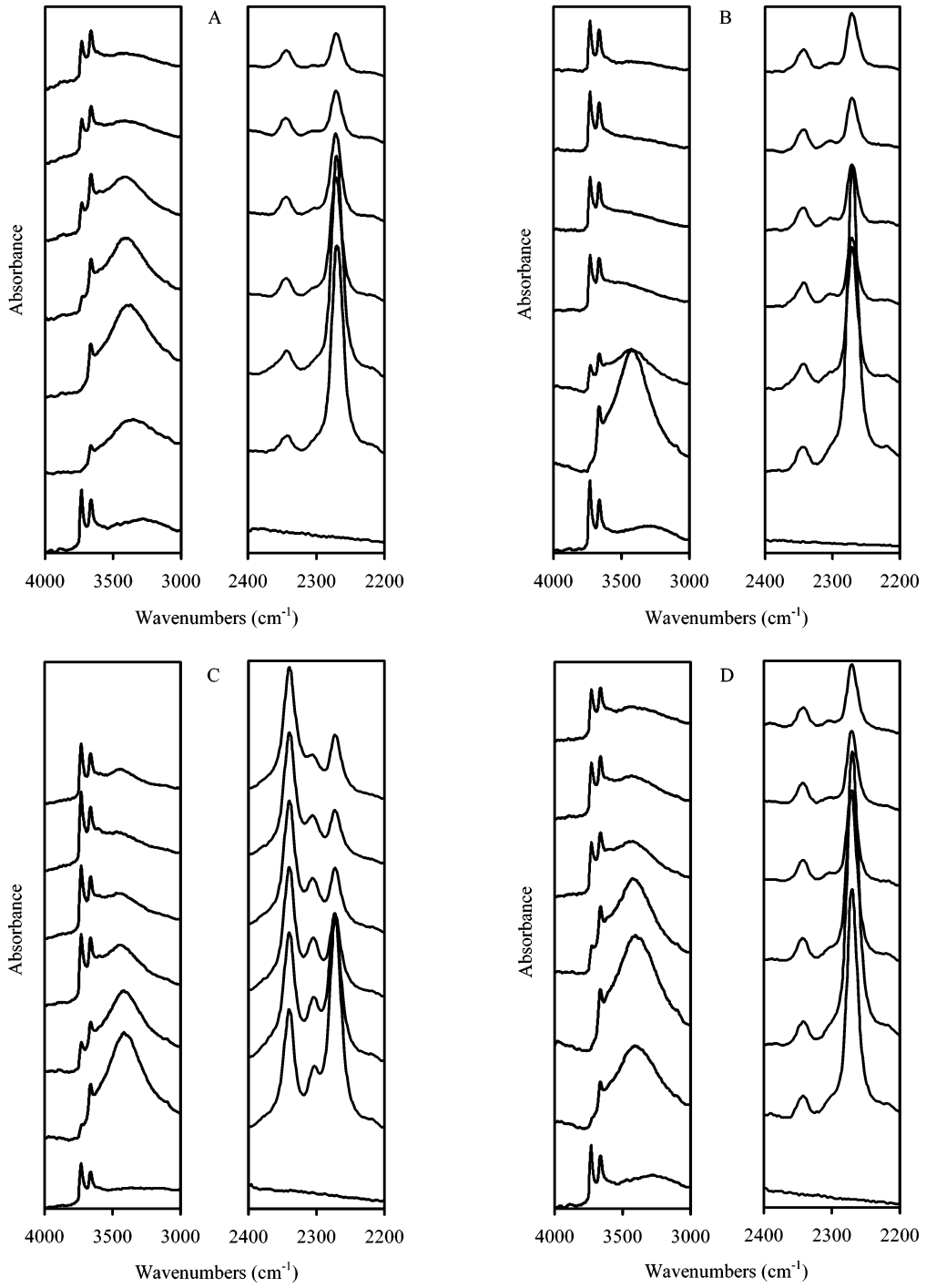

Figure 3. DRIFT spectra (2200−2400 and 3000−4000 cm^{-1}) of (A) FSMSap H^+, (B) FSMSap $NaAlO_2$ H^+, (C) FSMSap $Al(NO_3)_3$ H^+, and (D) FSMSap $Al(i\text{-}C_3H_7O)_3$ H^+ before (lowest spectra) and after reaction with CD_3CN at desorption temperatures increasing with 50 °C from 50 to 300 °C (upper spectra).

temperature results in the disappearance of the signal at 3734 cm^{-1} due to bridging hydroxyl groups and to the development of signals at 2114 (not shown), 2272, 2305, and 2341 cm^{-1}. According to literature data,[24,26,27] the different signals can be assigned to the stretching vibrations of CD_3 groups ($\nu(CD_3)$, signal at 2114 cm^{-1}) and to ν(CN) vibrations of deuterated acetonitrile interacting with Brønsted (signal at 2272 cm^{-1}) and Lewis (signal at 2341 cm^{-1}) sites, while the band at 2305 cm^{-1} could be assigned to exposed Mg^{2+} ions, in surface defects. The signal at 3668 cm^{-1} due to the octahedral Mg_3OH groups seems hardly to be involved in the interaction of the acetonitrile, only diminishing very little after adsorption of CD_3CN. A new broad band centered at about 3450 cm^{-1} also becomes visible in the spectra. Outgassing at increasing temperatures restores progressively the original spectrum. These results show that silanol groups (Si−OHs) exposed on the external surface in edges and/or defect sites interact with CD_3CN, while most of the Mg_3OH groups in the lattice are not accessible and do not interact. The adsorption of the probe on the Al-FSMSap H^+ samples at room temperature revealed a rather weak interaction of the base with the surface, since the band characteristic of the interaction with Brønsted sites was shifted to 2272 cm^{-1}. The latter was in fact constituted of two components, one at 2275 cm^{-1} due to interaction with Brønsted sites and the second at 2268 cm^{-1} attributed to acetonitrile interacting with the surface by weak hydrogen bonding, more likely with silanol

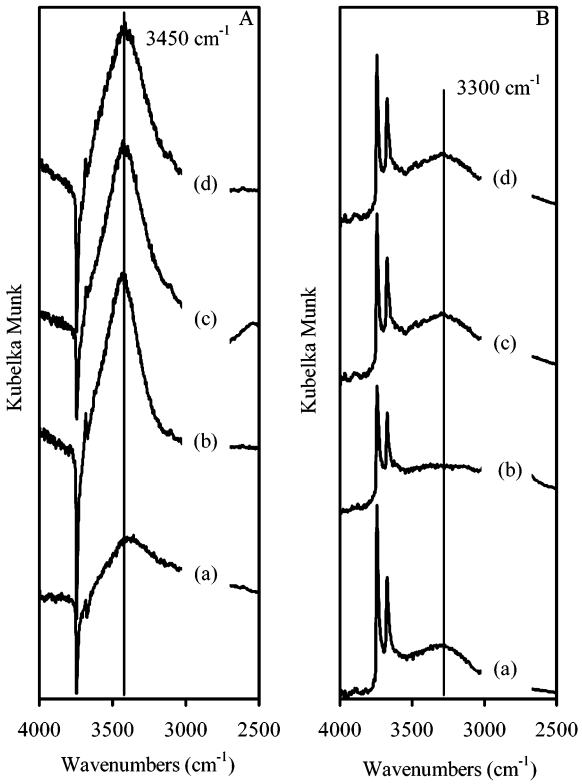

Figure 4. (A) Subtraction DRIFT spectra (2500−4000 cm^{-1}) relative to the adsorption of CHA on (a) FSMSap H^+, (b) FSMSap $NaAlO_2$ H^+, (c) FSMSap $Al(NO_3)_3$ H^+, (d) FSMSap $Al(i\text{-}C_3H_7O)_3$ H^+, and (B) DRIFT spectra (2500−4000 cm^{-1}) after outgassing at a temperature of 300 °C.

groups. The stability of the corresponding species under desorption is, as expected, stronger the higher the corresponding CN stretching frequency. At higher temperatures the band assigned to the Brønsted sites shifted to 2275 cm^{-1}, the CD_3CN interaction being stronger compared to the interaction with the silanols. After desorption at 300 °C, the base interacting with silanol groups was totally removed from the surface, while the signals characterizing Brønsted and Lewis sites were retained.

The band at 2305 cm^{-1} (exposed Mg^{2+} ions), was the most intense for the FSMSap $Al(NO_3)_3$ H^+ sample (Figure 3C). This could be attributed to the lowering of pH of the reaction mixture prepared using the aluminum nitrate source consequently creating some surface defects. Apparently, their intensity was heavily diminished in function of the temperature pointing out that these sites were quite weakly acidic. On the other samples the amount of adsorbed CD_3CN on those sites was almost not detectable, since due to the silting up of the residual clay after synthesis and the subsequent irreversible collapse of the clay after calcination, very little defect surface sites were present.

To better visualize the differences in the spectra, the spectrum of the acid-activated samples are subtracted from the spectra recorded after acetonitrile adsorption. These difference spectra provide evidence for the structural perturbations arising from the adsorption: negative bands represent species on the activated surface that disappear or are perturbed upon adsorption; positive bands are due to species formed upon adsorption. In Figure 4A the subtraction spectra relative to the adsorption of CD_3CN on the Al-FSMSap samples are reported. The very weak negative band at 3668 cm^{-1} confirms the almost total inaccessibility of the Mg_3OH groups. It is evident that the perturbation of the surface OHs is, due to the reaction of the free silanols, responsible for the strong negative band at 3734 cm^{-1}. In fact, for all samples the band at 3450 cm^{-1}, due to silanols hydrogen-bonded with acetonitrile, is present as a positive feature. Additionally, as detailed in the DRIFT spectra in Figure 4B, a broad medium intensity component centered near 3300 cm^{-1} was found after outgassing at 300 °C. No such broad band was obtained for Al-free materials. This component is much more intense than the band at 3450 cm^{-1}, especially after outgassing, than after contact with the gas. So, the component in the region 3400−2800 cm^{-1} is due to species resisting outgassing more than that responsible for the component at 3450 cm^{-1}, and formed only on Al-containing samples. Therefore, a certain part of the negative band at 3734 cm^{-1} in the difference spectra, representing a fraction of silanols that are stronger interacting with CD_3CN than the silica silanols, results in a positive feature at 3300 cm^{-1} present as a weak shoulder of the component at 3450 cm^{-1}. This broad low-frequency feature must be assigned to the OH stretching of hydrogen-bonded complexes of CD_3CN with a fraction of silanols that are stronger Brønsted acids than the silica silanols, and they must be present more abundantly on the surface of Al-rich samples. However, one cannot take it for granted that the Brønsted acid sites are strong if no ABC contour like for the acidic H−ZSM-5 is observed in the subtraction DRIFT spectra.

These results fully agree with those reported several years ago by Rouxhet and co-workers,[28,29] recently explained by Trombetta et al.,[30] for amorphous materials that clearly showed that acidic and nonacidic OHs on silica−aluminas are terminal and are responsible for a single band when free, but interact differently with bases. The authors concluded that the Brønsted acidic sites and the less acidic "normal" silanols, present also on silicas, are indistinguishable from the point of view of IR spectroscopy, when free. However, they behave differently upon adsorption of bases, giving rise to stronger H-bonding interactions with weak bases such as CD_3CN. This is not surprising, since the O−H stretching frequency is a property of the undissociated and unperturbed "acid" species, while its acidity (depending on the ΔG of dissociation) is a relative property of the "acid" with respect to its conjugated base (dissociated species). In agreement with basic general chemistry,[31] the stabilization of the conjugated base is a main factor allowing strengthening of the acidity, more than some kind of "activation" of the acid itself. These conclusions are consequently to be extended to mesoporous materials.

An estimation of the relative amount and the strength of the Brønsted and Lewis acid sites could be performed at a desorption temperature of 200 °C, all the physisorbed acetonitrile being removed. Integrating the DRIFT spectra in Kubelka−Munk units at 2272 cm^{-1}, one could conclude that the ratio of the Brønsted sites to Lewis sites increased in the order of FSMSap H^+ < FSMSap $Al(NO_3)_3$ H^+ < FSMSap $NaAlO_2$ H^+ < FSMSap $Al(i\text{-}C_3H_7O)_3$ H^+, while the Lewis acidity remained almost constant for all the Al-FSMSap H^+ samples except for the FSMSap $Al(NO_3)_3$ H^+ sample possessing a remarkably larger Lewis acidity. Moreover, more Brønsted than Lewis sites were present in all the Al-FSMSap H^+ samples except for the FSMSap $Al(NO_3)_3$ H^+ sample. Finally, the order of the total acidity of the samples, estimated from the total amount of adsorbed acetonitrile, confirms the results obtained via the adsorption of the strong basic probes (CHA, NH_3).

Determination of the Aluminum Coordination. The ^{27}Al NMR spectra are potentially very helpful for probing the quantity, coordination, and location of aluminum atoms in aluminosilicates, since X-ray diffraction only elucidates the long-range order of these materials. Nevertheless, the quadrupolar

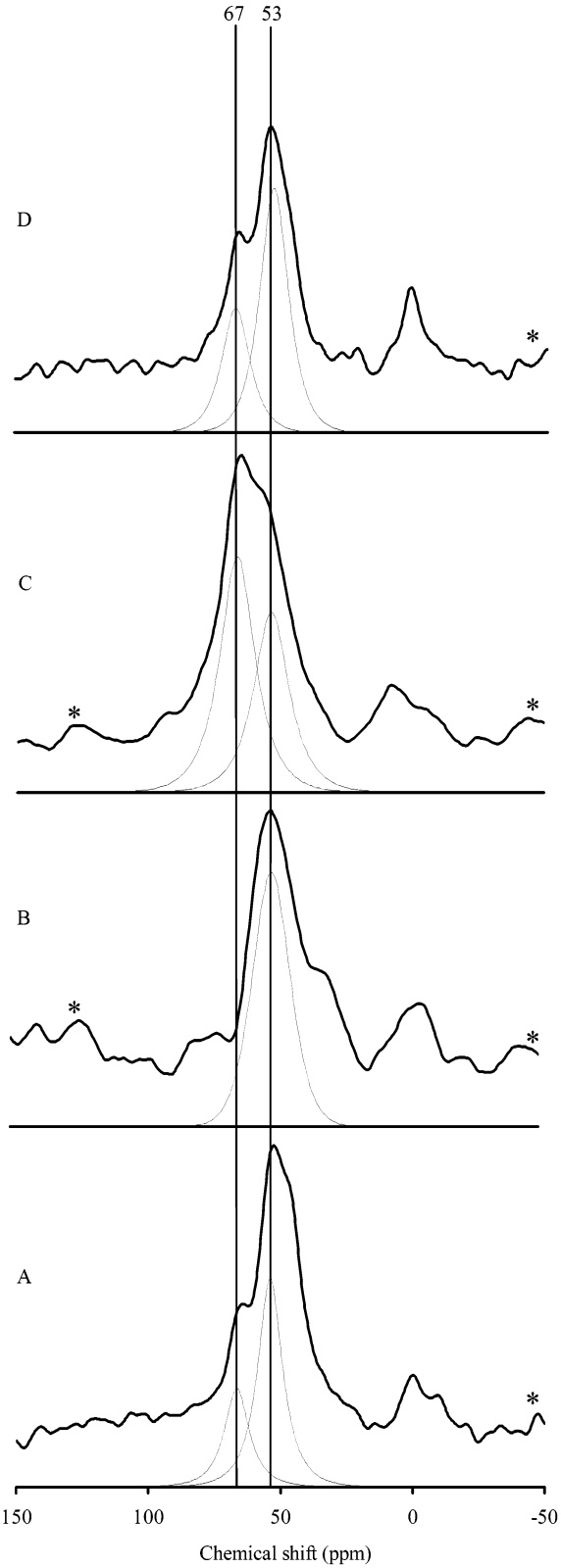

Figure 5. ^{27}Al MAS NMR spectra and deconvolution on the principal two peaks around 60 ppm of (A) FSMSap H^+, (B) FSMSap $NaAlO_2$ H^+, (C) FSMSap $Al(NO_3)_3$ H^+, and (D) FSMSap Al(*i*-$C_3H_7O)_3$ H^+.

nature of the nucleus does not allow the observation of the structurally significant fine structure of the bands, limiting the applicability of ^{27}Al MAS NMR to little more than the determination of the coordination number at the aluminum atom.

Bearing in mind that the final synthesized and acidified material consists of the Al-FSMSap H^+ sample and a residual fraction of leached Saponite, the NMR spectra in Figure 5 are clarified, the peaks being listed in Table 3. As determined in existing literature, the natural Saponite (from Ballarat, California) shows only one ^{27}Al peak centered at 67 ppm (not shown), in the region corresponding to tetrahedrally coordinated aluminum (Al^{IV}), confirming the absence of aluminum atoms in the octahedral sheet.[32,33] The ^{27}Al NMR spectra of the Al-FSMSap H^+ samples are clearly dominated by the signal in the range around 60 ppm, which is characteristic of tetrahedrally coordinated (framework) Al sites. The small resonances on either side of the principal resonance, indicated in Figure 5 with an asterisk, are spinning sidebands, which are due to partial averaging of the quadrupolar interactions.[34] Exact positions and relative areas of the spectral components were calculated by spectral deconvolution. The signals at 67 and 53 ppm are both due to tetrahedrally coordinated aluminum, respectively present in the residual Saponite and the mesoporous aluminosilicate (in which aluminum is covalently bound to four Si atoms via oxygen bridges). Mean values of deconvolution data obtained by several different fitting strategies show that, for the original FSMSap H^+ and the FSMSap Al(*i*-$C_3H_7O)_3$ H^+ sample, $^1/_3$ of the Al^{IV} originates from the leached clay while $^2/_3$ is incorporated into tetrahedral framework positions of the mesoporous sample. The FSMSap $NaAlO_2$ H^+ sample showed no peak at 67 ppm, pointing out that almost all the tetrahedral aluminum is derived from the incorporation of the aluminum into tetrahedral framework positions of the mesoporous structure. In the FSMSap $Al(NO_3)_3$ H^+ sample however, about 60% of the Al^{IV} originates from the Saponite, while only 40% is incorporated into the mesoporous structure. The presence of a residual leached clay fraction was already observed by XRD analysis at high angles 2θ and IR measurements and is now confirmed by Al^{27}-NMR. The spectra of the FSMSap H^+ and the FSMSap $NaAlO_2$ H^+ sample showed, in addition to the peaks attributed to tetrahedral and octahedral aluminum, additional shoulders at different chemical shift values. According to various authors[32,35,36], these peaks can be attributed to aluminum in a highly distorted tetrahedral coordination. In all cases, the presence of octahedrally coordinated (nonframework) aluminum is also indicated by the comparably weak signal in the region around 0 ppm. The broad asymmetric Al^{VI} NMR peak indicates multiple octahedral-site environments, being sensitive to different substitutions.[37] The respective relative peak intensities are calculated by spectral deconvolution and listed in Table 3. Assuming that the concentration of the tetrahedral and octahedral aluminum are proportional to the respective intensities of the resonances in the range around 60 and 0 ppm, it is observed that the ratio of aluminum in the tetrahedral to that of aluminum in the octahedral environment (Al^{IV}/Al^{VI}) increases in the order of FSMSap H^+ < FSMSap $NaAlO_2$ H^+ < FSMSap Al(*i*-$C_3H_7O)_3$ H^+ < FSMSap $Al(NO_3)_3$ H^+. The relative peak intensities, as calculated in Table 3, further verify that $AlNO_3$ is superior in comparison to the other aluminum sources in

TABLE 3: Results of the Deconvolution of ^{27}Al MAS NMR Spectra of the Al-FSMSap H^+: Relative Portions (%) of Different Coordinated Al Sites

coord.[a]	type	FSMSap H^+	FSMSap $NaAlO_2$ H^+	FSMSap $Al(NO_3)_3$ H^+	FSMSap Al(*i*-$C_3H_7O)_3$ H^+
Al^{IV}	clay	17	0	49	28
	FSM	37	63	36	54
	dist.[b]	30	20	0	0
		84	83	85	82
Al^{VI}		16	17	15	18

[a] Coordination. [b] Distorted.

providing the highest amount of acid sites and higher concentrations of tetrahedral aluminum for FSMSap aluminum incorporation.

Conclusion

The acidic Al-FSMSap samples, synthesized via a new successful short time synthesis route using leached saponite and a low concentration of surfactant, are thoroughly investigated. The resulting aluminosilicate mesoporous materials with high Si/Al ratios of around 11 have a maximal surface area of 1130 m^2/g, a pore volume of 0.92 cm^3/g, and a narrow pore size distribution at around 3 nm. These materials have been additionally incorporated with aluminum utilizing sodium aluminate, aluminum nitrate, and aluminum isopropoxide. The replacement of the sodium ions, present as counterions in the synthesized aluminosilicates, with protons imparted useful catalytic acidity. This acidity is extensively evaluated with FTIR spectroscopy after adsorption of ammonia and cyclohexylamine. All samples were highly acidic, though Al-FSMSap incorporated with aluminum nitrate is the most optimal having up to 1.3 mmol acid sites per gram. Apparently, the determination of the amount of adsorbed cyclohexylamine with thermogravimetrical analysis was a reliable technique for the quantification of the surface acid sites of the samples. By investigation of the nature of the acid sites with in situ IR spectroscopy after adsorption of acetonitrile, it is found that in all samples except the one incorporated with $Al(NO_3)_3$ more Brønsted than Lewis sites are present, both sites being of medium acidic strength as they resist desorption temperatures up to 300 °C. Probing the coordination and location of the Al atoms ^{27}Al MAS NMR confirmed that most of the aluminum in the Al-FSMSap materials is in tetrahedral positions. For the proton-exchanged $Al(NO_3)_3$ incorporated sample, even 95% of the total Al amount was found to be tetrahedral.

Acknowledgment. T. Linssen is indebted to the IWT for financial support. P. Cool acknowledges the FWO Vlaanderen (Fund for Scientific Research-Flanders-Belgium) for financial support.

References and Notes

(1) Kresge, C. T.; Leonowicz, M. E.; Roth, W. J.; Vartuli, J. C.; Beck, J. S. *Nature* **1992**, *359*, 710.
(2) Inagaki, S.; Fukushima, Y.; Kuroda, K. *J. Chem. Soc., Chem. Commun.* **1993**, *8*, 680.
(3) O′Brien, S.; Francis, R. J.; Price, S. J.; O'Hare, D.; Clark, S. M.; Okazaki, N.; Kuroda, K. *J. Chem. Soc., Chem. Commun.* **1995**, 2423.
(4) Mokaya, R. *J. Chem. Soc., Chem. Commun.* **2000**, 1891.
(5) Corma, A.; Fornés, V.; Navarro, M. T.; Pérez-Pariente, J. *J. Catal.* **1994**, *148*, 569.
(6) Kosslick, H.; Lischke, G.; Parlitz, B.; Storek, W.; Fricke, R. *Appl. Catal. A* **1999**, *184*, 49
(7) Reddy, K. M.; Song, C. *Catal. Lett.* **1996**, *36*, 103.
(8) Inagaki, S.; Yamada, Y.; Fukushima, Y. In *Progress in Zeolite and Microporous Materials, Studies in Surface Science and Catalysis*; Chon, H., Ihm, S.-K., Uh, Y. S., Eds.; Elsevier: Amsterdam, 1997; Vol. 105, p 109.
(9) Kan, Q.; Fornés, V.; Rey F.; Corma, A. *Mater. Chem.* **2000**, *10*, 993.
(10) Linssen, T.; Barroudi, M.; Cool, P.; Vansant, E. F. In *Zeolites and Mesoporous Materials at the Dawn of the 21st Century, Studies in Surface Science and Catalysis*; Galarneau, A., Di Renzo, F., Fajula, F.; Vedrine, J., Eds.; Elsevier: Amsterdam, 2001; Vol. 135, pp 6−15.
(11) Sayari, A. *Chem. Mater.* **1996**, ***8***, 1480.
(12) Mokaya, R.; Jones, W. *J. Chem. Soc., Chem. Commun.* **1996**, 983.
(13) Corma, A.; Grande, M. S.; Gonzales-Alfaro, V.; Orchilles, A. V. *J. Catal.* **1996**, *159*, 375.
(14) Linssen, T.; Cool, P.; Baroudi, M.; Cassiers, K.; Vansant, E. F.; Lebedev, O.; Van Landuyt, J. *J. Phys. Chem. B* **2002**, *106*, 4470.
(15) Linssen, T.; Cassiers, K.; Cool, P.; Vansant, E. F.; Lebedev, O. *Chem. Mater.* **2003**, submitted.
(16) Inagaki, S.; Yamada, Y.; Fukushima, Y. *Stud. Surf. Sci. Catal.* **1997**, *105*, 109.
(17) Kan, Q.; Fornés, V.; Rey, F.; Corma, A. *J. Mater. Chem.* **2000**, *10*, 993.
(18) Zhao, D.; Nie, C.; Zhou, Y.; Xia, S.; Huang, L.; Li, Q. *Catal. Today* **2001**, *68*, 11.
(19) Koch, H.; Böhmer, U.; Klemt, A.; Reschetilowski, W.; Stöcker, M. *Faraday* **1998**, *94*, 817.
(20) Breen, C. *Clay Miner.* **1991**, *26*, 487.
(21) Polverejan, M.; Liu, Y.; Pinnavaia, T. J. *Chem. Mater.* **2002**, *14*, 2283.
(22) Lambert, J. F.; Poncelet, G. *Top. Catalysis* **1997**, *4*, 43.
(23) Busca, G. *Phys. Chem. Chem. Phys.* **1999**, *1*, 723.
(24) Jolly, S.; Saussey, J.; Lavalley, J. C. *Catal. Lett.* **1994**, *24*, 141.
(25) Pelmenschikov, A. G.; van Santen, R. A.; Jänchen J.; Meijer, E. *J. Phys. Chem.* **1993**, *97*, 11071.
(26) Trombetta, M.; Busca, G.; Lenarda, M.; Storaro, L.; Ganzerla, R.; Piovesan, L.; Lopez, A. J.; Alcantara-Rodriguez, M.; Rodriguez-Castellon, E. *Appl. Catal. A* **2000**, *193*, 55.
(27) Chiche, B.; Sauvage, E.; Di Renzo, F.; Ivanova, I. I.; Fajula, F. *J. Mol. Catal. A: Chem.* **1998**, *134*, 145.
(28) Sempels, R. E.; Rouxhet, P. G. *J. Colloid Interface Sci.* **1976**, *55*, 263.
(29) Scokart, P. O.; Rouxhet, P. G. *J. Colloid Interface Sci.* **1982**, *80*, 96.
(30) Trombetta, M.; Busca, G.; Lenarda, M.; Storaro, L.; Pavan, M. *Appl. Catal. A* **1999**, *182*, 225.
(31) Cotton, F. A.; Wilkinson, G. *Advanced Inorganic Chemistry*, 4th ed.; Wiley: New York, 1980; Chapter 6.
(32) Storaro, L.; Lenarda, M.; Perissinotto, M.; Lucchini, V.; Ganzerla, R. *Micropor. Mesopor. Mater.* **1998**, *20*, 317.
(33) Woessner, D. E. *Am. Mineral.* **1989**, *74*, 203.
(34) Fyfe, C. A.; Thomas, J. M.; Klinowski, J.; Gobbi, G. C. *Angew. Chem., Int. Ed. Engl.* **1983**, *22*, 259.
(35) Chaudhari, K.; Das, T. K.; Chandwadkar, A. J.; Sivasanker, S. *J. Catal.* **1999**, *186*, 81.
(36) Lambert, J. F.; Millman, W. S.; Fripiat, J. J. *J. Am. Chem. Soc.* **1989**, *111*, 3517.
(37) Woessner, D. E. *Am. Mineral.* **1989**, *74*, 203.